Synthetic Aperture Radar Imagery Analysis and Applications Using SOCET GXP®

Afonso Martins Duarte
afonso.duarte@tecnico.ulisboa.pt

Instituto Superior Técnico, Lisboa, Portugal

May 2021

Abstract

Synthetic Aperture Radar (SAR) has been extensively used for remote sensing of the Earth for a few decades. It provides high resolution images in an all weather, day and night fashion for a multitude of applications. With the advances in RADAR technology, more and more data is generated and needs to be analysed and processed. The main purpose of this dissertation is to provide a reader who is interested in SAR imagery a good starting point to get accustomed to application oriented SAR data processing and visualization. This goal is achieved using BAE SYSTEMS SOCET GXP® software tool. The document provides the reader with key SAR concepts (imaging modes, product levels, polarisations, etc) followed by various simulations of some of the tool's features in real world applications as well as several use cases. The obtained results present a solid approach to the novice analyst by using the tool for the exploitation of SAR images as a source for geospatial information and data regarding water resource detection, terrain feature extraction, vegetation health assessment among other applications.
Keywords: Synthetic Aperture Radar, Image Processing, Image Visualization, Feature Extraction, BAE SYSTEMS SOCET GXP®

1. Introduction

If one was asked to condense in a single word what Electrical Engineering is all about, RADAR would probably be a very good candidate. Its composition involves all the intricate parts that make up an engineering student's career such as signal processing, electromagnetism, microwaves and so forth. But when it comes to the real world, these are merely sub parts of some type of system that actually possesses an actual, useful application. And here is where RADAR comes into play.

When we mention to RADAR we are usually referring to a RAR where the antenna is a physical object that first emits, and then collects, radiation. In this particular case we are going to be covering SAR systems where the antenna is in motion in order to cover a synthetic aperture, hence its designation and acronym. These systems possess a diverse quiver of applications such as remote sensing, surface mapping and foliage penetration. By taking a brief look at this short list, one can without difficulty think of a multitude of applications where SAR might be applied. Ranging from topography and oceanography to monitoring infrastructure stability and even military surveillance, the opportunities are virtually endless making this specific topic one of the utmost importance to explore and, hopefully, provide better solutions to be implemented on future telecommunication systems involving the use of SAR systems and specifically data processing and visualization tools.

2. Overview

This technique provides high resolution with the remarkable characteristic that its resolution does not degrade with distance. Distance weakens the strength of the radar reflections and can increase image noise, but resolution cell size does not increase as distance increases.

Other advantages of working with SAR technology include the ability to extract different features from different bands of operation at which one collects data from a specific physical location. Consequently, this action will result in heavy amounts of SAR data in more or less fine resolutions. Independently of what the case may be, a few options are available referring to what tools can one use to visualize, analyze and process the vast amount of data that can be collected by any probe or sensor. This will be the main focus of this work.

3. Objectives

It is certain that SAR technology has much to offer. With several satellite constellations already in operation as well as multiple airborne sensors currently in operation, there is plenty of data to be processed and analysed. With this goal in mind, several software tools were considered (both for personal and commercial use) and eventually, one was chosen to tackle the task. Ultimately, we will be addressing SOCET GXP® in an attempt to expose the capabilities of such tool as well as the kind of information that can be extracted using it when working with SAR imagery from any kind of source. A few use cases will also be presented with the intent of providing a good starting point for anyone interested in beginning to work with SAR data, particularly when it comes to processing, visualization and feature extraction.

4. Background

A Radar is an sensor which is sensible enough to detect and locate electromagnetic waves which are reflected by other objects. Firstly, it radiates energy in the form of electromagnetic waves from an antenna which then propagate in a given medium. Secondly, some of this radiated energy collides with a reflecting object, which is usually called a *target*, and is located at a certain distance from the radar. Next, as this energy collides with the target, it is re-radiated in multiple directions. Some of these directions happens to be the one of the receiver antenna and is perceived as echo. Finally, through amplification and adequate signal processing, a decision is made at the output of the receiver as to whether or not a target echo signal is present and allows us to determine the target location as well as some other useful information. [1]

4.1. The Radar Equation

We can now translate these parameters such as radiated and received energy into measurable entities and establish a relation between them. With this purpose in mind, it is now time to bring up the famous and governing, Radar Range Equation, widely known as simply Radar Equation. With it, it is possible not only to compute an estimate of the range of a certain system as a function of its characteristics but also to use it as a great starting point for designing a radar system:

$$P_r = P_t G_A \left(\frac{1}{4\pi |r_s|^2}\right) \sigma \left(\frac{1}{4\pi |r_s|^2}\right) A_e \tag{1}$$

which becomes:

$$P_r = \frac{P_t G_A A_e \sigma}{(4\pi)^2 |r_s|^4 L_{radar} L_{atmos}} \tag{2}$$

where:

- P_r = Received signal power (W)
- P_t = Transmitter signal power (W)
- G_A = Transmitter antenna gain factor
- A_e = Receiver antenna effective area (m^2)
- σ = Target Radar Cross Section (m)
- r_s = Range vector from target to the antenna (m)
- L_{radar} = Transmission loss factor due to miscellaneous sources
- L_{atmos} = Atmospheric loss factor due to the propagating wave

4.2. Radar Cross Section (RCS)

The Radar Cross Section of a given target literally reflects its ability to transmit energy back to the radar. For the specific case of SAR systems, the target of interest in terms of radar performance is generally a widespread, distributed target, such as plain fields with open areas, areas with dense foliage and vegetation or even metropolitan environments. Of course, for this target type, the RCS is dependent on the area being scanned and processed. Thus, for distributed targets, it is useful to specify RCS in terms of a 'reflectivity' unit that quantifies RCS per unit area and so, the actual area is the area of a resolution cell, as projected on the ground:

$$\sigma = \sigma_0 \delta_{cr} \left(\frac{\delta_r}{cos\Psi}\right) \tag{3}$$

where:

- σ_0 = Target reflectivity (m^2/m^2)
- δ_{cr} = Crossrange resolution (m)
- δ_r = Range resolution (m)
- Ψ = Grazing angle at target location

4.3. SAR State of the Art

As mentioned before, and unlike regular RADAR systems, SAR systems allow us to acquire imagery in the most challenging of circumstances and scenarios such as at night or under harsh atmospheric conditions. The aim is always to achieve a finer resolution whether we are airborne or spaceborne. Thanks to SAR, we can now take advantage of the long-range propagation characteristics of radar signals and the complex information processing capability of modern digital electronics to provide high resolution imagery.

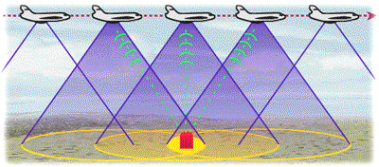

Figure 1: Example of an antenna on a moving platform - Quora

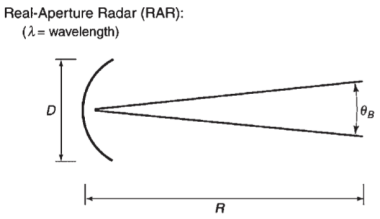

Figure 2: Diagram of a real aperture antenna - SciTech Publishing, Inc

SAR systems produce two-dimensional (2D) images, one dimension being range or the resolution along the line-of-sight from the radar to the target region and the second dimension being the crossrange (or azimuth) resolution or the resolution along the direction perpendicular to the LOS and parallel to the ground.

SAR's ability to produce relatively fine azimuth resolution makes it stand out from the crowd. Usually, to obtain fine crossrange resolution, a physically large antenna is needed to focus the transmitted and received energy into a sharp beam. The sharpness of the beam defines the crossrange resolution. Likewise, optical systems, such as telescopes, require large apertures (mirrors or lenses which are analogous to the radar antenna) to obtain fine imaging resolution. Since Synthetic SAR is much lower in frequency than optical systems, even moderate resolutions require an impractically large antenna to be carried by an airborne platform: antenna lengths of several hundred meters long are often required. However, airborne radar can collect data while flying this distance, and then process the data as if it came from a physically long antenna. [2]

The distance the aircraft flies in synthesizing the antenna is known as the synthetic aperture. A narrow synthetic beam width results from the relatively long *synthetic* aperture, which yields finer resolution than is possible from a smaller physical antenna. [3]

4.4. Real and Synthetic Aperture

Crossrange resolution was initially achieved using a narrow beam. Its width in radians of an aperture antenna is given approximately by the wavelength divided by the aperture diameter. The corresponding linear crossrange resolution at range R is then:

$$\delta_{cr} \approx \frac{R\lambda}{D} \tag{4}$$

or, in other words, a *real aperture.*

Now, if we move the platform of this physical antenna along a path in space we would, in principle, be able to achieve a crossrange resolution comparable to what would be achieved in a scenario where a real aperture antenna would have a length equal to the path length, thus making it a *synthetic aperture*, L_{SA}:

$$\delta_{cr} \approx \frac{R\lambda}{2L_{SA}} \approx \frac{\lambda}{2\Delta\theta} \tag{5}$$

where $\Delta\theta$ is the synthetic aperture angle, as seen from the target area. The additional factor of 2 occurs due to signal processing.

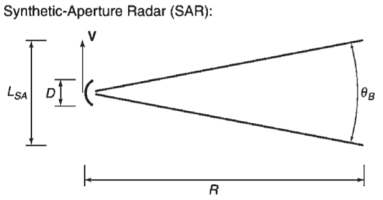

Figure 3: Diagram of a synthetic aperture antenna - SciTech Publishing, Inc

4.5. Range Resolution

Range provides an indication of the size of the smallest object identifiable in a particular acquired image. When it comes to *range resolution*, and in order to introduce the concept in an simpler way, we will resort to a step-frequency waveform which consists on a train of identical pulses of width τ. The phase and amplitude of each pulse echo is intercepted by the radar. After application of several Fourier Transforms, and noting that each pulse has a width of $1/B$ (bandwidth B) and the same for the sampling time interval:

$$\delta_r = \frac{c}{2B} \tag{6}$$

with the multiplication by $c/2$ since an incremental delay Δt corresponds to an incremental downrange distance of $c\Delta t/2$. The resolution is thus given in terms of pixel separation. [4]

4.6. Crossrange Resolution

Crossrange resolution, or *azimuth*, corresponds to the resolution along the direction perpendicular to

the LOS and parallel to the ground and increases with range. If we assume that the SAR is moving at a constant altitude H, speed V and time T along a direction perpendicular to the LOS we can state that $L_{sa} = VT$ and very small in comparison with the range R to the target area. With this taken in due consideration, and using (5):

$$\delta_{cr} = \frac{\lambda}{2\Delta\theta} \approx \frac{\lambda R}{2L_{SA}} = \frac{\lambda R}{2VT} \tag{7}$$

4.7. Data Acquisition

At each crossrange position along a certain trajectory, the moving SAR broadcasts pulses and is aware of the respective echoes. This information is then stored in the shape of a two-dimensional array of complex numbers consisting of magnitude and phase (see fig:prodinfochain for the data flow). If we process this data as a function of downrange and crossrange it is possible to render a radar image.

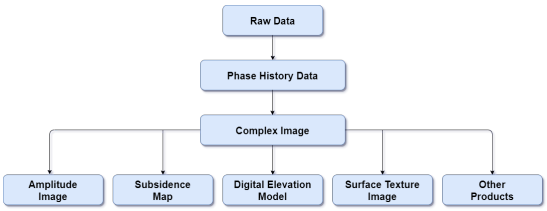

Figure 4: The SAR product formation chain

The acquisition system can be defined through the following three frequencies.

The first one corresponds to the oscillator frequency (f_c) (the radar's carrier frequency, defining the wavelength):

$$\lambda = \frac{c}{f_c} \tag{8}$$

The second one defines the length of a range pixel through the sampling frequency. As the radar measures slant range, the ground range pixel is the projection of the slant range pixel on the ground. For the echo of a pulse to be sufficiently sampled, f_d must be larger than the pulse modulation bandwidth (which determines the instrument resolution). The range resolution of the acquired data is thus finer than the instrument resolution:

$$p_d = \frac{c}{2f_d} \tag{9}$$

Finally, and no less relevant, the third frequency pertains to pulse repetition (f_a) which, along with the SAR's velocity v, will dictate the crossrange (or azimuth) resolution of the acquired data. In other words, the length of a crossrange pixel:

$$p_a = \frac{v}{f_a} \tag{10}$$

4.8. Data Processing

Obtaining high-resolution images involves three-dimensional processing which is comprised of two stages: range and azimuth compression.

Next, a Digital Elevation Model (DEM) is used to measure the phase differences between the acquired complex arrays, which is determined from different acquisition angles to discern the height information. This height information, along with the crossrange coordinates provided by two-dimensional SAR focusing, will provide the third dimension, which is elevation. The reflected signal that is captured by the receiving antenna is a significantly lower, attenuated power and time-shifted version of the original signal, the latter being our reference signal.

While performing *range compression*, the received signal is correlated with the reference signal with the result being the information on the target's range. This is also referred to as a *matched filter* which consists in the application of a Fast Fourier Transform to both signals, multiplying the two and then performing a reverse transform on this product.

Finally, *crossrange compression* is applied also using a *matched filter*, but performed in the azimuth direction for each range bin. [4]

4.9. SAR Bands of Operation

Optical sensors collect data in the visible, near infrared, and short wave infrared portions of the electromagnetic spectrum. RADAR sensors on the other hand, such as the case of SAR, make use of longer wavelengths at the centimeter to meter scale, which confers it with unique properties such as the ability to see through clouds as mentioned. When it comes to dealing with SAR systems, the different operating wavelengths are often referred to as bands by letter designations such as X, C, L and P for instance.

Wavelength is an important feature to consider when working with SAR, as it determines how the RADAR signal interacts with the surface and how far a signal can penetrate into a medium. For instance, an X-band RADAR, which operates at a wavelength of about 3 cm, has very little capability to penetrate into broadleaf vegetation, and consequently, interacts with leaves at the top of the tree canopy most of the time. An L-band signal, on the other hand, has a wavelength of about 23 cm, achieving greater penetration into vegetation and allowing for more interaction between the RADAR signal and large branches or tree trunks (see figure 5). Wavelength also impacts penetration into other land cover types such as soil and ice.

4.10. Imaging Modes

When it comes to acquiring imagery, different SAR sensors will feature different imaging mode varia-

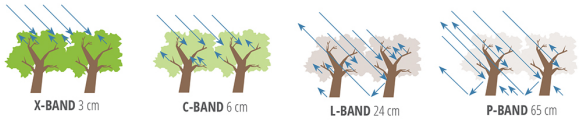

Figure 5: Sensitivity of SAR measurements to forest environment and depth of vegetation penetration at different wavelengths - NASA SAR Handbook.

tions. Despite of this fact, it is possible to state, on a more general perspective, three main imaging modes present in most sensors, each sensor with its specific variations: Stripmap mode, Spotlight mode and ScanSAR mode.

4.11. Stripmap Imaging Mode

In Stripmap mode is commonly known as the basic SAR imaging mode. The ground swath is illuminated with a continuous sequence of pulses while the antenna beam is fixed in elevation and azimuth. This results in an image strip with a continuous image quality in the direction of flight (see figure 6). In order to achieve a consistent ground range resolution that matches the azimuth resolution, the transmitted pulse bandwidth is tuned specifically for each collection and is heavily dependent on the incidence angle.

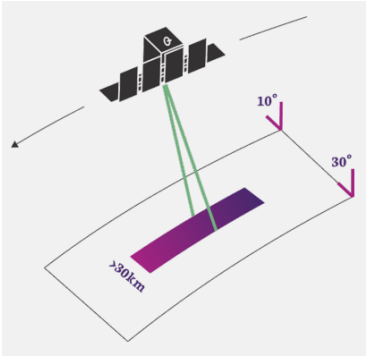

Figure 6: Illustration of the Stripmap SAR Imaging Mode - ICEYE SAR Product Guide.

4.12. Spotlight Imaging Mode

In Spotlight mode, the RADAR beam is constantly steered towards an aim point on the ground (see figure 7). This increases the time that the target area is illuminated, resulting in an increased synthetic aperture, and therefore, better azimuth resolution compared to a continuous stripmap mode.

As is the case of Stripmap mode, slant plane image resolution will also vary according to the transmitted pulse bandwidth and the this product is also then translated into a ground plane image.

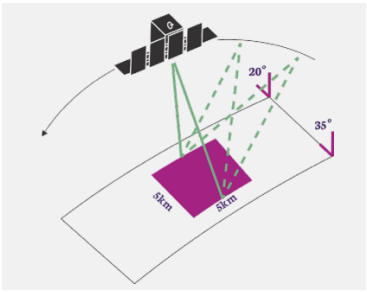

Figure 7: Illustration of the Spotlight SAR Imaging Mode - ICEYE SAR Product Guide.

4.13. ScanSAR Imaging Mode

In the ScanSAR imaging mode, electronic antenna elevation steering is used to acquire adjacent, slightly overlapping coverage areas with different incidence angles that are processed into one scene (see figure 8). For systems such as TerraSAR-X for example, a swath width of 100 km or more is achieved by scanning four adjacent ground sub-swaths with quasi-simultaneous beams, each with different incidence angle. There are also other more advanced modes that allow for wider swath values which is the case of WideScanSAR [5].

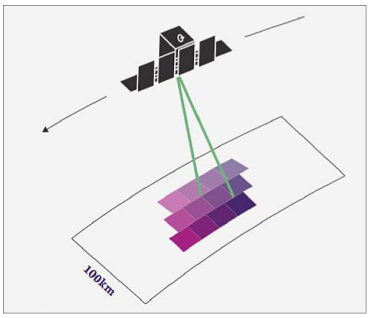

Figure 8: Illustration of the ScanSAR Imaging Mode - ICEYE-X2.

4.14. Rules of Thumb for SAR Image Interpretation

At this stage, it is convenient to present some general rules when analysing SAR imagery. These tips are meant to aid the reader in quickly spotting and extracting relevant information from any data in use.

1. Regions of calm water and other smooth surfaces will appear black, because the incident RADAR reflects away from the spacecraft.

2. Surface variations near the size of the RADAR's wavelength cause strong backscattering.

3. A rough surface backscatters more brightly when it is wet.

4. Wind-roughened water can backscatter brightly when the resulting waves are close in size to the incident RADAR's wavelength.

5. Hills and other large-scale surface variations tend to appear bright on the side that faces the sensor and dim on the side that faces away from the sensor. Mountains show this effect to the extreme, in part due to increased foreshortening.

6. Due to the reflectivity and angular structure of buildings, bridges, and other human-made objects, these targets tend to behave as corner reflectors and show up as bright spots in a SAR image.

7. A corner reflector can look like a bright cross in a processed SAR image since it is a particularly strong response.

4.15. SOCET GXP® Tool Characterization

While an enormous effort has been expended on systems to acquire SAR data, in comparison, little has been made with the intent of making the best use of said data. Software tools such as SOCET GXP® aim to solve this issue by bridging what we know about the data and the best way to get to and extract the relevant information they contain.

Despite the extent of an analyst's ability, it is a very time consuming task to extract the information and specially when large areas are concerned. Moreover, we are unable to guarantee consistency between studies if we don't know what tools to use, how they differ or how well they perform in a specific case or application. These limitations drive the exploration of these tools in an effort to derive relevant information more quickly and in a way that is reproducible.

5. SAR Tool Capabilities

When it comes to the format of the acquired data, for every piece of energy sent to the ground, two values are received: magnitude which is the amount of energy that gets reflected and phase which expresses the time that that energy took to return to the sensor. Next, these values come off the sensor as I and Q which represent complex numbers. SOCET GXP® then converts the sensor independent complex data into magnitude and phase when the data is loaded. Finally, the data is divided into three main image components in a hierarchical fashion:

- Raw phase history data which comes directly from the sensor

- Complex imagery containing magnitude and phase information from sensor and is formed from raw phase data

- Detected imagery where only the magnitude is represented and formed from complex imagery. Has the disadvantage of missing valuable information such as time and depth.

5.1. Data Limitations

It is important to note that the amount of features and relevant information that can be extracted and inferred from a particular set of data is limited to the quality (or "richness", so to speak) of that specific dataset. The metric of quality should be expressed in terms of the user's intent. Some dataset characteristics (imaging mode, polarisation, type of sensor, acquisition distance and duration, acquisition bands, etc...) might not be suitable for the user's intended purpose.

Throughout the course of this work, the selected data and results stem from the available datasets at the time of writing. Ideally, specific data should be requested for a particular location of interest. The process of requesting and obtaining such data is often not available to the general public and may not be accessible free of charge. For the purposes of this dissertation, the original idea was to obtain a proper data set from the Yucatán Peninsula in southeastern Mexico but since said data was not delivered in a timely manner, the presented work was performed using sample data from multiple sources such as L3HARRIS™, ICEYE, AIRBUS and MAXAR.

5.2. Histogram Features

By taking advantage of the distribution of the image pixel values, we're able to use the histogram features built-in. The histogram tool dismisses pixel values equal or close to zero and "stretches" the remaining values to then obtain a brighter, sharper image. The thresholds at which this cut-off is performed can be adjusted in the Lower and Upper percentage cut-off inputs. This panel shows the number of times a particular pixel value occurs in the image where the horizontal axis indicates the pixel value and the vertical axis denotes the number of pixels at that particular value.

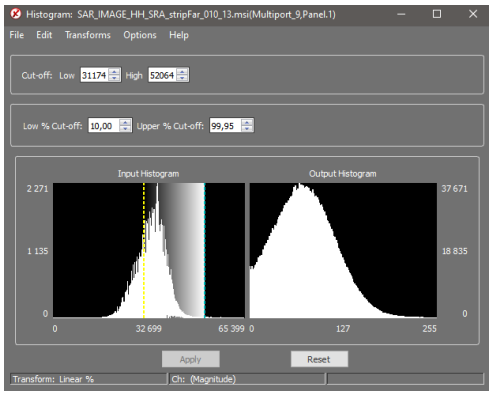

Figure 9: Image histogram using SOCET GXP®.

The input histogram on the left in figure 9 displays the histogram for the raw data where a low digital number is shown as a black color in the image and a high digital number appears white. Upon opening an image file, it is automatically remapped and the results of this remapping are shown in the output histogram on the right. Of course, the result of the histogram changes whenever the user "looks" to a different region within the image. This specific feature is one of the ways of determining certain terrain characteristics such as water resources, for example, by exploiting the distinct pixel signature inherent to the RADAR signal response of water.

5.3. Threshold LUT

Look Up Tables allow users to map pixels of certain values or ranges to other various colors. The Threshold LUT functionality modifies the pixels of an image according to a defined percentage. For example, we may choose to display a specific band by itself and display a percentage of the brightest pixels present in that particular band:

Figure 10: Threshold values at: 0 (left), 50 (center), 99 (right) using SOCET GXP® (Lake Constance, Germany).

For instance, when we set the threshold value to 99 (see figure 10), only the top 1% of pixels remain on display which can be useful for detecting hotspots (as in the highest pixel values). If we are presented with a landscape and we aim to find out where in that landscape a specific element (like clay, for example) is more heavily present, we know that in that particular band is where clay is going to spike and is often the only present signature after applying this LUT threshold.

5.4. Width and Height Measurements

It is also possible to quickly measure features and objects on imagery (see figure 11 and figure 12). Let us suppose that we wish to measure the width of a plot of land. We can make use of the acquired data and the tool to determine its width accurately. The height of a building can also be determined.

5.5. Multi-Spectral Imagery Classification

Traditional 4-band Multi-Spectral Imagery contains bands of red, green, blue and near-infrared. Each band can be assigned to any of the R, G, or B channels displayed on the Multiport®. Upon obtaining compatible data, true-color imagery is what the human eye sees which results from assigning the red, green and blue bands to their respective red, green and blue channels. With MSI imagery we can assign bands to different RGB values in order to highlight items or regions of interest such as healthy or dying vegetation, for example. And the more bands we have available within the dataset, the more combinations can be displayed. Let us take a look at an example of Rio de Janeiro's coastal area in Brazil.

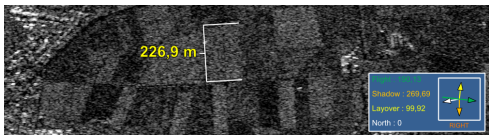

Figure 11: Farmland plot width measurement using SOCET GXP® (Lake Constance, Germany).

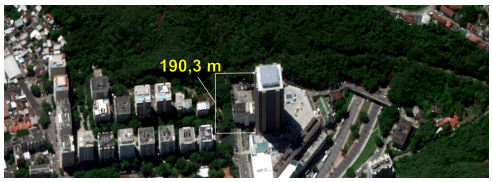

Figure 12: Building height measurement using SOCET GXP® (Rio de Janeiro, Brazil).

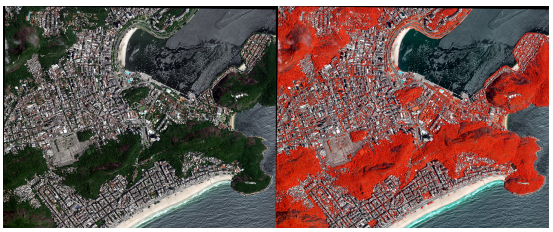

Figure 13: Band filtering with near-infrared selection at 833 nm wavelength using SOCET GXP® (Rio de Janeiro, Brazil).

As is evident in figure 13, we can observe the effects of spectral selection on areas with certain types of vegetation and/or in certain conditions. The different red color gradients serve as an indicator of whether or not vegetation in a particular area is well watered/healthy or not. Proper quantification can also be performed by taking a look at the exact magnitude values shown by these particularly highlighted areas.

5.6. Spectral Angle Mapper

The Spectral Angle Mapper functionality falls within the Supervised Classification category where algorithms are used to match in-scene pixels to an existing spectral signature.

The classification is supervised in the sense that it is the user who selects the pixels to find in the scene and the algorithms to identify similar pixels

Figure 14: Supervised classification of vegetation, roads and water using SOCET GXP® (Tripoli, Libia).

which account for each band in the image. In this type of classification, the angle between vectors created by two spectral signatures is measured. Figure 14 shows an example of the output product using Spectral Angle Mapping supervised classification of vegetation (in green), roads (in red) and water (in blue). This feature presents itself as yet another way of estimating vegetation area. Moreover, we can also make use of spectral libraries where a list of materials with known spectral signatures is present. With this information, one can, for example, find in the scene evidence for the presence of certain types of vegetation such as Willow Sedge, Whitebark Pine, Lodgepole Pine among other species of commonly found vegetation.

5.7. Colorization

Detecting the presence of water on any given surface is an essential application. It prevents the actual, physical inspection of the site in question and further debate as to whether or not to select that particular location for farmland or reject it as an unreliable construction site. By taking advantage of the colorization features of SOCET GXP® we are able to tell with reasonable accuracy the location of water resources such as rivers, creeks and ponds.

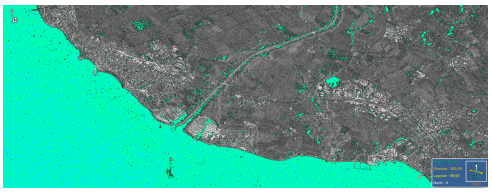

Figure 15: Water resource detection through colorization using SOCET GXP® (Lake Constance, Germany).

The results shown in figure 15 were obtained by locking in the spectral signature of the large body of water surrounding the region and then assigning a particular color (in this case, a cyan green gradient) to areas where the complex signal values are similar. It is also important to note that the figure shows a juxtaposition of two sets of imagery from the same site, the first acquired in HH polarization and the second in VV polarisation

6. Use Cases

Due to the limitations in 5.1, we will still address real world scenarios but since we are unable to use the intended tool with the desired data, we will instead make use of the existing literature to exemplify some of the intended use cases using as reference publications that can be found in [6] and [7].

6.1. Soil Moisture Estimation

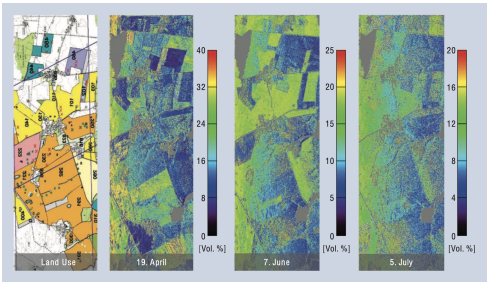

Figure 16: Soil moisture maps obtained after applying polarimetric decomposition to remove the vegetation layer and inverting the remaining ground component - IEEE Geoscience and Remote Sensing Magazine.

In figure 16, we can visualize the soil moisture maps obtained from polarimetric L-band SAR data acquired at three different dates. At the time of the first acquisition in April, the crop layer was still short and light. Its height and density increased during the next acquisitions performed in June and July. If we were to use SOCET GXP® as originally planned, we would be able to produce similar results involving moisture gradients which would then translate into practical values pertaining to soil moisture volume in percentage as depicted.

6.2. Subsidence Estimation

Figure 17 shows the subsidence over Mexico City estimated with two TerraSAR-X images acquired with a 6 month difference. We can observe that the maximum displacement is about 15 cm in some city areas. The subsidence is due to ground water extraction and it is a well-known problem in Mexico City. Provided that we could have access to such data, similar results could also be obtained using SOCET GXP®. By taking advantage of the temporally spaced RADAR acquisitions in addition to the topographic information as well as reflectivity and phase information it would be possible to simulate a similar subsidence map, albeit with different color gradients.

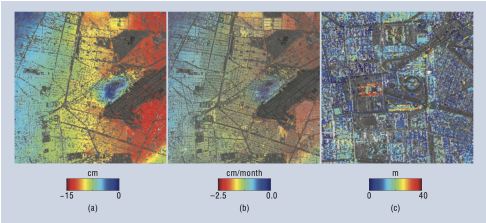

Figure 17: (a) Estimated subsidence over Mexico City (overlay of reflectivity and phase) (b) Mean deformation velocity estimated over Mexico City (c) Zoom over the city of the refined DEM. The scene size is approximately 8 km x 8 km. RADAR illumination from the right - IEEE Geoscience and Remote Sensing Magazine.

6.3. Forest Height Estimation

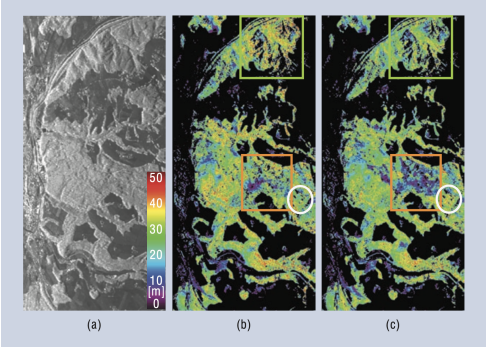

Figure 18: (a) L-band HV intensity image of the Traunstein test site. Forest height map computed from Pol-InSAR data in (b) 2003 and (c) 2008 - IEEE Geoscience and Remote Sensing Magazine.

In figure 18, an L-band SAR image of the Traunstein forest site, located in southern Germany is shown. The Traunstein forest is characterized by a large variety of forest stand conditions in the presence of locally variable topography. In the middle and on the right of the figure we can visualize forest height maps derived from Pol-InSAR data acquired at L-band in 2003 (b) and 2008 (c).

Comparing the two forest height maps a number of changes within the forest become visible: The logging of individual tall trees as a result of a change in forest management between 2003 and 2008 (marked by the green box); the damage caused in January 2007 by the hurricane Kyrill which blew down large parts of the forest (marked by the orange box); and finally forest growth on the order of 3 to 5 m over young stands as seen within the area marked by the white circle. In the context of this work, the selected tool could be used to obtain similar maps either taking advantage of the Colorization features (see 5.7), Multi-Spectral features (see 5.5) or even Spectral Angle Mapping (see 5.6) for more accurate results.

6.4. Oil Spill Detection

SAR images can also be extremely useful when detecting oil spills. Oil pollution from sea-based sources can be accidental or deliberate. Whatever the case may be, oil is a major threat to the sea ecosystems and SAR is of very great use in mitigating this issue. The possibility of detecting an oil spill in a SAR image relies on the fact that the oil film decreases the backscattering of the sea surface resulting in a dark formation that contrasts with the brightness of the surrounding spill-free water.

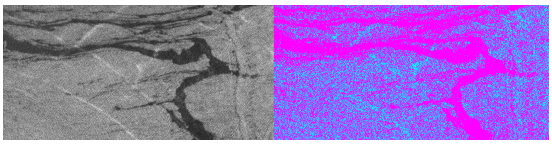

Figure 19: Original oil spill SAR image (left) and post-classification SAR image (right) - International Oil Spill Response Technical Seminar.

In figure 19 we can observe the 2010 Dalian Xingang oil spill event in Japan. From the original SAR image, the darker areas correspond to the oil contents in the ocean. This particular example was selected since it wielded the most resemblance to the results that would be obtained in SOCET GXP® with the adequate data and using Colorization (see 5.7) in conjunction with Spectral Angle Mapping (see 5.6) or even Threshold LUTs (see 5.3). The article does not mention from which sensor the data originated neither its acquisition mode or polarisation.

7. Conclusion

Throughout the course of this work we sought to achieve two main goals:

1. Find a SAR imagery analysis tool that could deliver prompt and useful results from virtually any relevant imagery source
2. Provide a hands-on approach to SAR imagery analysis with the aid of the aforementioned tool.

Upon exploring and evaluating some of the existing tools, SOCET GXP® fulfilled the intended purpose with distinction, specially considering the data that was available at the time of writing and its limitations (refer to 5.1). This document is primarily targeted to readers new to the use of SAR imagery and who want to gain relevant insight on what first steps to take in order to begin exploring the possibilities of SAR while producing relevant outputs without having to spend huge amounts of time looking into the technicalities of RADAR imaging before being able to deliver useful results.

7.1. Future Work

Furthering this work will undoubtedly be dependent on the richness of data, how adequate and available said data is in relation to its intended application and also on further advances when it comes to SAR imaging technology and processing. The current generation of SAR instruments is, however, limited in their capability to acquire RADAR images with both high-resolution and wide-swath coverage. This immediately impacts the acquisition frequency if large contiguous areas shall be mapped systematically with a single satellite. The resolution versus swath width restriction is fundamental and closely connected to the intricacies of the SAR data acquisition process. Taking that and other factors into context, the future SAR development landscape will likely be impacted by:

1. Increased **data availability** specially when it comes to ease of access and "richness"
2. Further developments when it comes to **advanced imaging techniques**

7.2. Data Availability

Despite the fact that some previously restricted SAR datasets are becoming more available (such as the sample imagery datasets used in this document), these do not carry the full spectrum of possibilities from a user standpoint that is not part of the commercial sphere as is the case here. A shroud of secrecy is still present and, although justifiable or understandable in part, it hinders further advances on behalf of the general public. On the bright side, there are upcoming missions promising multi-band data and advocating free and open data policies. These will greatly benefit the public archive of RADAR imagery of the Earth.

7.3. Advanced Imaging Techniques

Several SAR imaging modes have been developed that provide different trade-offs between spatial coverage and azimuth resolution. Examples are the ScanSAR mode (see 4.13), which enables a wide swath at the cost of an impaired azimuth resolution, and the Spotlight mode (see 4.12), which allows for an improved azimuth resolution at the cost of a non contiguous imaging along the satellite track. However, it is not possible to combine both imaging modes and to overcome this issue, several innovative digital beamforming techniques have been presented where the receiving antenna is split into multiple sub-apertures that are connected to individual receiver channels. A good example is the currently under development high-resolution wide-swath (HRWS) SAR at EADS Astrium [8]. The system has been specified to map a 70 km wide swath with a resolution of 1 m, thereby exceeding the number of acquired ground resolution cells of the TerraSAR-X Stripmap mode (3 m resolution at 30 km swath width) by a factor of 21.

7.4. Final Remarks

In an ever changing and dynamic world, geospatial information with global access and coverage becomes more and more important. Constellations of spaceborne satellites as well as airborne sensors play a major role in this task considering that SAR is the only all weather, day and night sensor. With the various applications already mentioned, the future for SAR remote sensing looks promising. Tools like the one used in this work alongside wide data availability originating from sensors equipped with highly innovative concepts hereby mentioned will allow the global observation of dynamic processes on the Earth's surface with unparalleled quality and resolution. It will open the door to a future global remote sensing system with high resolution imagery and relevant geospatial information updated by the minute.

Acknowledgements

The author would like to thank Prof. António Topa as well as Jay Gordon and Diego Balcázar over at BAE SYSTEMS for making this work come into fruition. This dissertation had as its host institution, the Telecommunications Institute (Instituto de Telecomunicações).

References

[1] M. Skolnik. *Introduction to Radar Systems*. New York: McGraw-Hill, 2nd edition, 2001.

[2] T. Freeman. What is Imaging Radar? Website. NASA Jet Propulsion Laboratory.

[3] M. Skolnik. *Radar Handbook*. New York: McGraw-Hill, 3rd edition, 2008.

[4] L. J. Cutrona. *Radar Handbook*, chapter Synthetic Aperture Radar. New York: McGraw-Hill, 2nd edition, 1990.

[5] AIRBUS. *TerraSAR-X Image Product Guide - Basic and Enhanced Radar Satellite Imagery*.

[6] Alberto Moreira. A Tutorial on Synthetic Aperture Radar. *IEEE Geoscience and Remote Sensing Magazine*, March 2013.

[7] Jianchao Fan. Oil Spill Monitoring based on SAR Remote Sensing Imagery. *Aquatic Procedia 3 - International Oil Spill Response Technical Seminar*, pages 112 – 118, 2015.

[8] Federica Bordoni, Marwan Younis, N. Gebert, Gerhard Krieger, and Christian Fischer. Performance Investigation on the High-Resolution Wide-Swath SAR System with Monostatic Architecture. pages 1122–1125, 06 2010.